# Negative Ion Density Fronts during Ignition and Extinction of Plasmas in Electronegative Gases

I. D. Kaganovich, D. J. Economou, B. N. Ramamurthi, and V. Midha

*Department of Chemical Engineering, University of Houston, 4800 Calhoun Road, Houston, Texas 77204-4792*

Negative ion density fronts have been shown to occur in electronegative *steady-state* plasmas with hot electrons. In this Letter, we report theoretical and numerical results on the spatiotemporal evolution of negative ion density fronts during plasma *ignition* and *extinction* (afterglow). During plasma ignition, the negative ion fronts are analogous to hydrodynamic shocks. This is *not* the case during plasma extinction where, although negative ions diffuse freely in the plasma core, the negative ion front propagates towards the chamber walls with a nearly constant velocity.

PACS numbers: 52.35.Lv, 52.35.Tc, 52.75.Rx

Negative ion rich (electronegative) plasmas are of great importance in many fields, including semiconductor manufacturing [1], elimination of notching [2], negative ion sources [3], the ionospheric $D$ layer [4], etc. Electronegative plasmas with hot electrons ($T_e \gg T_i$, $T_e$ and $T_i$ are the temperatures of electrons and ions, respectively) often separate into an ion-ion core region, where negative ions segregate, and an electron-ion edge region (near the walls) which contains no negative ions [5]. Depending on conditions, a double layer may form separating the ion-ion core and the electron-ion regions. Negative ion density fronts and double layers have been shown to occur in steady-state collisionless [6] or collisional [7,8] plasmas. Formation of the fronts has been attributed to ion acoustic waves [9] for collisionless plasmas, or to direct currents passing through the plasma [10] for collisional plasmas. For collisional steady-state plasmas, we have shown [7] that the negative ion fronts are similar to hydrodynamic shocks [11]. However, the spatiotemporal evolution of negative ion densities and associated front formation have not been studied during ignition or extinction of electronegative plasmas. Such a study is reported in this Letter.

We focus on collisional plasma transport, where the ion mean free path is smaller than the plasma chamber dimensions. The presence of negative ions substantially influences the charged species fluxes in a plasma. Indeed, assuming a two-component (electrons and positive ions with densities $p = n_e$) plasma, and Boltzmann equilibrium for electrons, $E = -T_e/e\nabla(\ln n_e)$, the drift flux of positive ions is reduced to an effective linear (ambipolar) diffusion flux, $\mu_i pE = -\mu_i T_e\nabla n_e$. In a plasma containing negative ions (with density $n$, with $p = n + n_e$), however, the conventional ambipolar diffusion equation is no longer valid [10]. The ion flux is now described by a combination of diffusion and convection, with a velocity that depends nonlinearly on the ion and electron densities, e.g., the drift flux of positive ions is a nonlinear function of densities, $\mu_i pE = -\mu_i T_e p/n_e\nabla n_e$, which is the origin of the negative ion density fronts [5].

These negative ion density fronts have been observed experimentally in steady-state oxygen rf glow discharges sustained in capacitively coupled parallel plate reactors [12,13]. The negative ion density profile, measured by a Langmuir probe [14], tends to form a front at the electrode.

Negative ion fronts also exist during ignition and extinction (afterglow) of electronegative plasmas. The spatiotemporal evolution of such fronts is studied theoretically and by a numerical "experiment" in an argon/oxygen pulsed discharge. In pulsed discharges, power to the discharge is modulated (e.g., square wave modulation) with a specific frequency and duty ratio. During plasma ignition (power on), self-sharpening negative ion density fronts develop and move towards the plasma center, in analogy with hydrodynamic shocks. During the afterglow, negative ion fronts exist when $T_e \gg T_i$, and move towards the chamber walls. However, the latter fronts are of a completely different nature and have no direct analogy with hydrodynamic shocks. The propagation of hydrodynamic shocks is dominated by convection, and dissipative mechanisms (viscosity, thermal conductivity) influence only the internal shock structure. In contrast, for sufficiently high electronegativity, negative ions diffuse nearly freely and the role of drift is negligible. During the afterglow, negative ions diffusing freely in the ion-ion core, slow down as they approach the edge region due to increasing electrostatic field. The drift flux due to the field is directed towards the plasma center and, at the periphery, nearly compensates the diffusion flux, which is in the opposite direction.

The resulting negative ion velocity is directed outwards; it turns out that, although the main evolution is by diffusion, the negative ion front propagation speed is nearly constant for constant electron and ion temperatures. The negative ion front is a new type of nonlinear structure, different from hydrodynamic nonlinear waves, and beyond the classification of dissipative structures done in [15]. The evolution of ion fronts in the afterglow of electronegative plasmas is very important, since it determines the time needed for negative ions to reach the wall and thus influence surface reactions in plasma processing.

For a collisional plasma the particle fluxes are described by a drift-diffusion model, $\Gamma_k = -D_k \partial n_k/\partial x \pm \mu_k n_k E$, where $D_k$ and $\mu_k$ are the $k$-particle diffusion coefficient and mobility, respectively, tied by the Einstein relation

$D_k = T_k \mu_k$. $T_k$ is the $k$-particle temperature. The self-consistent electrostatic field can be found from the condition of zero net current $j = e(\Gamma_p - \Gamma_n - \Gamma_e) = 0$. If the electron density is not too small ($\mu_e n_e \gg \mu_i n, \mu_i p$), electrons are described by Boltzmann equilibrium, $E = -T_e/e \nabla(\ln n_e)$. Substituting the expression for electric field into the continuity equations for negative ions and electrons, and using the electroneutrality constraint, yields a complete system of equations,

$$\frac{\partial n}{\partial t} - \frac{\partial}{\partial x}\left(\mu_i T_i \frac{\partial n}{\partial x} - un\right) = \nu n_e - \gamma_d n - \beta_{ii} np,$$

(1a)

$$\frac{\partial n_e}{\partial t} - \frac{\partial}{\partial x}\left(D_{\text{eff}} \frac{\partial n_e}{\partial x}\right) = (Z_{\text{ioniz}} - \nu_{\text{att}})n_e + \gamma_d n,$$

(1b)

$$n_e = p - n,$$

$$u \equiv \frac{\mu_i T_e}{n_e}\frac{\partial n_e}{\partial x}, \quad D_{\text{eff}} \equiv \frac{\mu_i T_e(p + n)}{n_e} + \mu_i T_i, \quad (1c)$$

where, for simplicity, we have considered the case of equal ion mobilities and diffusion coefficients, $\mu_p = \mu_n \equiv \mu_i$, and $D_p = D_n \equiv D_i = \mu_i T_i$. In the above equations, $\beta_{ii}$ is the ion-ion recombination rate coefficient, and $Z_{\text{ioniz}}$, $\nu_{\text{att}}$, and $\gamma_d$, are the ionization, attachment, and detachment frequencies, respectively. We impose the Bohm velocity for positive ions at the plasma-sheath boundary [1] and zero negative ion density. The continuity [Eq. (1)] should be supplemented with an equation for the electron temperature [1]:

$$\frac{\partial}{\partial t}\left(\frac{3}{2} n_e T_e\right) + \frac{\partial q_e}{\partial x} = W - \sum_i R_i H_i, \quad (1d)$$

where $q_e = -\chi_e \partial T_e/\partial x + 2.5 T_e \Gamma_e$ is the electron heat flux, $W$ is power density deposited in electrons, and $R_i$ is the reaction rate of electron impact process $i$ with activation energy $H_i$. The boundary conditions are zero flux at the discharge center and $q_e = 2.5 T_e \Gamma_e$ at the plasma-sheath boundary. The simulation results using Eqs. (1) agreed nicely with experimental data for the steady-state plasma profiles [13].

The ion convective velocity $u$ [Eq. (1c)] is proportional to the gradient of the logarithm of the electron density. If the electron density were a given function $f(x)$, nonlinear phenomena would not appear. Nonlinear convection appears because the electron density gradient changes simultaneously with the negative ion density, due to the dependence of $D_{\text{eff}}$ [Eq. (1c)] on electronegativity ($n/n_e$). Substituting $\partial n_e/\partial x$ from the expression $\Gamma_e = -D_{\text{eff}} \partial n_e/\partial x$, and neglecting sources and sinks Eq. (1a) can be rewritten in the form,

$$\frac{\partial n}{\partial t} + \frac{\partial}{\partial x}\Gamma_n - \frac{\partial}{\partial x}\mu_i T_i \frac{\partial n}{\partial x} = 0,$$

$$\Gamma_n(n/n_e) = -\frac{n\Gamma_e}{n + p}.$$

(2)

Equation (2) shows explicitly that the convective flux of negative ions is a nonlinear function of the negative ion density. The velocity of density profile propagation $u_{\text{eff}} = \partial \Gamma_n/\partial n$ depends on the negative ion density $n$; the smaller the value of $n$, the larger the $u_{\text{eff}}$. Regions with small negative ion density move faster than regions with higher ion density. This means [7] that even if the initial negative ion density profiles are smooth, fronts will be formed, preferably in the regions where $n \approx 0$. The implication is that the plasma will segregate into an ion-ion core and an electron-ion periphery as a result of profile evolution.

In Fig. 1, negative ion ($O^-$) front formation is shown for the ignition (active glow) phase of an argon 97%–oxygen 3% pulsed discharge. The plasma profiles are described by the continuity [Eqs. (1a)–(1c)] coupled with an equation for the electron temperature (1d). The reaction coefficients are taken from [1]. The initial condition of the plasma at the beginning of the active glow corresponds to the final condition at the end of the afterglow. For the chosen set of parameters, this corresponds to an ion-ion plasma with smooth coslike profiles of charged species densities (lines for 0 $\mu$s). In the late afterglow, when electrons have almost disappeared, negative ions diffuse to the walls in the absence of significant electric fields. Once power is switched on (at time $t = 0$), the electron temperature rises up to several eV. As the electric field rises with electron temperature, negative ions are squeezed towards the center of the plasma. Since the (inward pointing) drift velocity is larger in regions of smaller negative ion density, a self-sharpening negative ion front develops (Fig. 1, 60 $\mu$s). This process continues until ion diffusion across the front counterbalances ion drift.

We have studied many different cases for both oxygen and chlorine discharges. The negative ion fronts are clearly seen during the active (power "on") glow if (1) the plasma electronegativity is not very small, $n/n_e > 1/2$, so that nonlinear terms are important, and (2) an edge region of
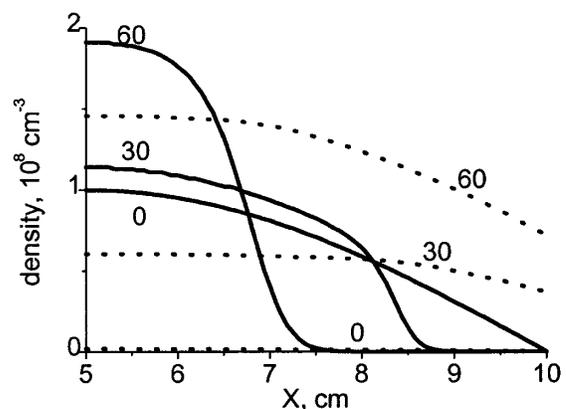


FIG. 1.   Negative ion (solid lines) and electron density (dashed lines) in the early active glow of Ar and 3% $O_2$ plasma. Inter-electrode gap: 10 cm; total pressure: 5 mTorr; averaged power density: 1.0 mW/cm$^3$; pulse duration: 600 $\mu$s; duty ratio: 0.5; numbers denote time in the active glow in $\mu$s.

electron-ion plasma exists, which corresponds to not very high electronegativity at the edge, $n/n_e < \sqrt{T_e/T_i}$ [8].

A new kind of negative ion fronts appear in the afterglow when $T_e \gg T_i$. High electron temperature in the afterglow can be due to two reasons: (1) superelastic collisions of electrons with metastable heat electrons, and (2) there can be a small residual power in the afterglow; in practical situations this may correspond to capacitively coupled biasing of an otherwise inductively coupled pulsed discharge; see, for example, [16]. Solving the heat conduction equation (1d) we found that a residual power as small as 0.1% of the power during the active glow can keep electrons warm with $T_e \sim 1$ eV. In the afterglow of a 97% Ar–3% $O_2$ we found that, initially, the electron temperature drops rapidly mainly due to electron impact excitation losses. Several $\mu$s into the afterglow, the electron temperature decreases from a value of 3.5 to $\sim 1$ eV with a residual power of only 0.1% of the power during the active glow. The electron impact excitation losses, which exponentially depend on $T_e$, switch off. Thus, the electron temperature remains high late in the afterglow.

In Fig. 2 the spatial profiles of densities and fluxes for both electrons (dashed lines) and negative ions (solid lines) are shown in the afterglow (50–200 $\mu$s after power is switched off), when the electron density is much smaller than the initial value of $4.2 \times 10^8$ cm$^{-3}$; the electron temperature was fixed at a value 1 eV in the afterglow. The electron density keeps decreasing mainly due to wall losses, while the total negative ion density remains nearly constant. Wall losses of negative ions are negligible when electrons with $T_e \gg T_i$ are still present. The electronegativity ratio $n/n_e$ is very large at the discharge center (ion-ion core) and approaches zero near the edge. Therefore, $D_{\text{eff}}$ [Eq. (1c)] is very inhomogeneous, large in the
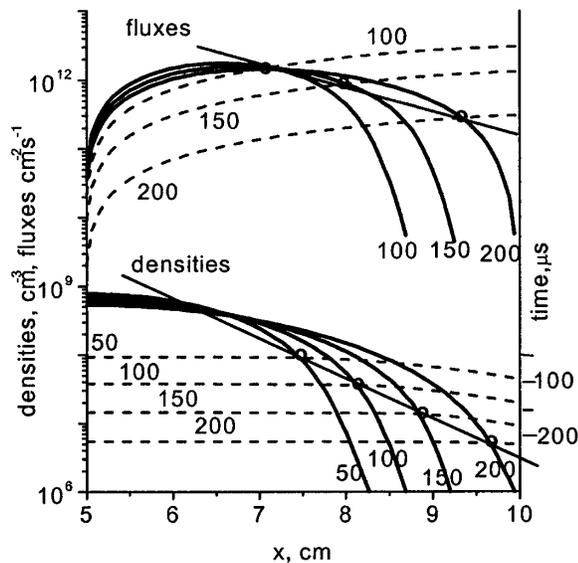


FIG. 2. Spatial profiles of fluxes and densities of negative ions (solid lines) and electrons (dashed lines) in the afterglow for the conditions of Fig. 1. The points where $\Gamma_n = \Gamma_e$ and $n_e = n$ are shown as circles; numbers denote time in the afterglow in $\mu$s.

ion-ion core region, $\approx \mu_i T_e n/n_e$, and small in the edge region, $\approx \mu_i T_e$.

The frequency of electron loss, $Z_{e,\text{loss}}$, which is determined by the slow diffusion in the edge region, is nearly constant as can be deduced from the exponential decay of electron density in Fig. 2. We have shown analytically that even though the ion-ion core with $L_{ii}(t)$ changes with time, $Z_{e,\text{loss}}$ varies insignificantly with $L_{ii}$. The negative ion motion is governed by the competition of diffusion and drift. In the ion-ion plasma core, $n \gg n_e$, $\Gamma_n \approx -\Gamma_e/2$, and Eq. (2) simplifies to

$$\frac{\partial n}{\partial t} = \frac{\partial}{\partial x}\left(D_i \frac{\partial n}{\partial x}\right) + \frac{1}{2}\left(Z_{\text{ioniz}}n_e - \frac{\partial n_e}{\partial t}\right). \quad (3)$$

Equation (3) is also valid at the steady state (with the time derivative terms set equal to zero). In the afterglow $Z_{\text{ioniz}} \approx 0$ and $\partial n_e/\partial t = -Z_{e,\text{loss}}n_e$. The frequency of electron loss $Z_{e,\text{loss}} = \mu_i T_{e,\text{aft}}\kappa^2$, and $Z_{\text{ioniz}} = \mu_i T_{e,\text{st}}\kappa^2$, where $T_{e,\text{st}}$ and $T_{e,\text{aft}}$ are electron temperatures at the steady state and the afterglow, respectively. Thus, at the very beginning of the afterglow, the first term on the right-hand side (rhs) of Eq. (3) is equal to the second term, and the negative ion density remains the same. When $T_e$ has quickly dropped several times due to inelastic processes, the second term on the rhs of Eq. (3) decreases, and the first term dominates. This implies that negative ions diffuse almost freely in this region and thus drift is small compared to diffusion. In the ion-ion plasma core ($n_e \ll n$), the positive and negative ion fluxes coincide (see Fig. 2).

As the negative ion density decreases towards the edge, the electric field increases, reducing the negative ion flux to practically zero. Thus, free ion diffusion is slowed down, since the electric field retards the motion of negative ions. As the electric field increases, the drift flux of negative ions equalizes the diffusive flux and, at some point, the net negative ion flux is reduced to $\Gamma_n \ll \Gamma_e$. At that point, negative ions are almost in Boltzmann equilibrium, $T_i(\partial n/\partial x) \approx T_e(n/n_e)(\partial n_e/\partial x)$. This implies that the negative ion density drops nearly exponentially, $n \sim \exp(-x/\delta)$, where $\delta = (T_i/T_e)[\partial \ln(n_e)/\partial x]^{-1}$, towards the edge plasma forming a negative ion front. The front can be seen clearly in Fig. 2.

The transition from nearly free negative ion diffusion (ion-ion core) to negative ion Boltzmann equilibrium occurs at the point where the diffusion flux becomes of the order of the drift flux. Therefore, the point where the negative ion density starts dropping rapidly can be estimated from the condition of equality of electron and ion fluxes $\Gamma_n = \Gamma_e$. Substituting expressions for fluxes $\Gamma_n = \mu_i T_i(\partial n/\partial x)$ and $\Gamma_e = xZ_{e,\text{loss}}n_e$, we find the equation for front propagation,

$$\mu_i T_i \frac{\partial n}{\partial x}\bigg|_{x_{if}} = Z_{e,\text{loss}}n_e x|_{x_{if}}. \quad (4)$$

The negative ion density profile in the ion-ion core can be found from Eq. (3) neglecting the second term in the

TABLE I. The ion front velocity ($10^4$ cm/s). $2L$ means the gap was increased by 2 times compared to the conditions of Figs. 1 and 2. $nW$ means the power was increased by $n$ times compared to the conditions of Fig. 2; for the case $100W$ oxygen percentage was 10%.

|            | $L$:$W$ | $L$:$2W$ | $L$:$10W$ | $L$:$100W$ | $2L$:$W$ | $2L$:$2W$ |
|------------|---------|----------|-----------|------------|----------|-----------|
| Simulation | 1.58    | 1.42     | 1.38      | 1.57       | 0.86     | 0.62      |
| Analytic   | 1.65    | 1.56     | 1.85      | 1.94       | 0.92     | 0.75      |

rhs. Assuming that negative ions diffuse a large distance compared to the initial extent of the ion-ion plasma core $L_{ii0}$, the solution of Eq. (3) for time $t > t_{ii} \equiv L_{ii0}^2/D_i$ is

$$n(x,t) = \frac{\int n(x,0)\,dx}{\sqrt{4\pi D_i \tau}}\, e^{-(x^2/4D_i\tau)}, \qquad (5)$$

where $\tau = t - t_{ii}$. Substituting $n(x,t)$ into Eq. (4) and $n_e(\tau) = n_e(t_{ii})\exp(-Z_{e,\text{loss}}\tau)$ we find

$$-\frac{x_{if}^2}{4D_i\tau} = -Z_{e,\text{loss}}\tau + \ln(B), \qquad (6)$$

where $B = Z_{e,\text{loss}}n_e(t_{ii})4\tau\sqrt{\pi D_i\tau}/\int n\,dx$. Free ion diffusion starts at time $t_{ii}$, when $D_i(\partial^2 n/\partial x^2) \sim 0.5 Z_{e,\text{loss}}n_e$, so that $B \sim 1$. Accordingly, for long times, $Z_{e,\text{loss}}\tau > 1$, Eq. (6) yields

$$x_{if} = V_{if}\tau, \quad \text{with } V_{if} = 2\sqrt{D_i Z_{e,\text{loss}}}. \qquad (7)$$

Surprisingly, the negative ion front moves with nearly constant velocity $V_{if}$. In Fig. 2 the points corresponding to $\Gamma_n = \Gamma_e$ (top) and $n_e = n$ (bottom) are shown. From this figure, one finds the velocity of the point at which $\Gamma_n = \Gamma_e$ as $2.6 \times 10^4$ cm/s, close to the analytic estimate [Eq. (7)] of $V_{if} = 3.2 \times 10^4$ cm/s. The velocity of the point at which $n_e = n$ is $1.6 \times 10^4$ cm/s, close to $V_{if}/2$. The velocity of the point at which $n_e = n$ is lower, since in this region $\Gamma_n < \Gamma_p$ (see Fig. 2), and the electric field retards ion free diffusion. We checked the velocity of propagation of the point at which $n_e = n$ for different discharge conditions. Interestingly, for all conditions, this velocity was close to $V_{if}/2$.

It is also interesting to note that the maximum velocity of negative ions, $V_{i,\max}$, is smaller than $V_{if}/2$. For example, for times $t = 50$, 100, and 150 $\mu$s, $V_{i,\max} = 0.7$, 0.8, and $0.97 \times 10^4$ cm/s, while $V_{if}/2 = 1.3 \times 10^4$ cm/s. The velocity of the negative ion front is different from the fluid velocity of negative ions at the position of the front. This is analogous to classical hydrodynamics, where the shock velocity is different from the velocities to the right and to the left of the shock [11]. In classical hydrodynamics, the shock velocity lies between these two velocities. We note that, in contrast to the negative ion fronts in the active glow, the velocity of the negative ion front in the afterglow is larger than the velocity of the negative ions everywhere in the discharge.

Table I shows that the phenomenon persists over a wide range of parameters. The necessary condition to clearly observe negative ion fronts is that negative ions are confined in the center of discharge, and negative ion density is not small, $n > \sim n_e$. For higher powers than in Fig. 2, nonlinear processes such as ion-ion recombination and detachment in collisions with metastables and oxygen atoms become important. As can be seen from Table I these processes do not affect negative ions much. The study of strongly electronegative gases where attachment is dominant in the afterglow (halogens) has shown that negative ion front movement can be affected by the production of negative ions in the edge region.

[1] M. A. Lieberman and A. J. Lichtenberg, *Principles of Plasma Discharges and Materials Processing* (Wiley, New York, 1994).
[2] G. S. Hwang and K. P. Giapis, Phys. Rev. Lett. **79**, 845 (1997).
[3] M. Hopkins and K. Mellon, Phys. Rev. Lett. **67**, 449 (1991).
[4] W. Swider, *Ionospheric Modeling* (Birkhauser Verlag, Basel, 1988).
[5] L. D. Tsendin, Sov. Phys. Tech. Phys. **34**, 11–15 (1989).
[6] V. Kolobov and D. Economou, Appl. Phys. Lett. **72**, 656 (1998).
[7] I. D. Kaganovich and L. D. Tsendin, Plasma Phys. Rep. **19**, 645 (1993).
[8] I. Kouznetsov, A. Lichtenberg, and M. Lieberman, J. Appl. Phys. (to be published); Plasma Sources Sci. Technol. (to be published).
[9] T. Takeuchi, S. Iizuka, and N. Sato, Phys. Rev. Lett. **80**, 77 (1998).
[10] A. P. Dmitriev, V. A. Rozhansky, and L. D. Tsendin, Sov. Phys. Usp. **28**, 467 (1985).
[11] G. B. Whitham, *Linear and Nonlinear Waves* (Wiley, New York, 1974).
[12] D. Vender, W. W. Stoffels, E. Stoffels, G. M. W. Kroesen, and F. J. de Hoog, Phys. Rev. E **51**, 2436 (1995).
[13] U. Buddemeier, Ph.D. thesis, Ruhr Universitaet, 1997.
[14] V. A. Godyak and R. B. Piejak, Phys. Rev. Lett. **65**, 996 (1990).
[15] B. S. Kerner and V. V. Osipov, Sov. Phys. Usp. **33**, 679 (1990).
[16] L. J. Overzet, Yun Lin, and L. Luo, J. Appl. Phys. **72**, 5579 (1992).